Amino Acids (2012) 42:2067–2077
DOI 10.1007/s00726-011-0938-7

ORIGINAL ARTICLE

# Peptides derived from *Mycobacterium tuberculosis* Rv2301 protein are involved in invasion to human epithelial cells and macrophages

**M. Ocampo · D. M. Rodríguez · H. Curtidor · M. Vanegas · M. A. Patarroyo · M. E. Patarroyo**

Received: 14 January 2011 / Accepted: 9 May 2011 / Published online: 19 May 2011


**Abstract** The specific function of putative cut2 protein (or CFP25), encoded by the *Rv2301* gene from *Mycobacterium tuberculosis* H37Rv, has not been identified yet. The aim of this study was to assess some of CFP25 characteristics and its possible biological role in *Mycobacterium tuberculosis* H37Rv invasion process to target cells. Molecular assays indicated that the gene encoding Rv2301 is present and transcribed in *M. tuberculosis* complex strains. The presence of Rv2301 protein over the bacilli surface was confirmed by Western blot and immunoelectron microscopy analyses, using goats sera inoculated with synthetic peptides derived from Rv2301 protein. Receptor–ligand binding assays with carcinomic human alveolar basal epithelial cells (A549) and macrophages derived from human histolytic lymphoma monocytes (U937) allowed us to identify five high activity binding peptides (HABPs) in both cell lines, and two additional HABPs only in A549 cells. U937 HABPs binding interactions were characterized by saturation assays, finding dissociation constants ($K_d$) within the nanomolar range and positive cooperativity ($n_H > 1$). Inhibition assays were performed to assess the possible biological role of Rv2301 identified HABPs, finding that some of them were able to inhibit invasion at a 5 μM concentration, compared with the cytochalasin control. On the other hand, HABPs, and especially HABP 36507 located at the N-terminus of the protein, facilitated the internalization of fluorescent latex beads into A549 cells. These findings are of vital importance for the rational selection of Rv2301 HABPs, to be included as components of an antituberculosis vaccine.

**Keywords** *Mycobacterium tuberculosis* · High activity binding peptides · Cutinase · Rv2301

M. Ocampo (✉) · D. M. Rodríguez · H. Curtidor · M. Vanegas · M. A. Patarroyo · M. E. Patarroyo
Fundación Instituto de Inmunología de Colombia (FIDIC), Carrera 50 No. 26-20, Bogotá, Colombia
e-mail: marisol.ocampo@urosario.edu.co

M. Ocampo · D. M. Rodríguez · H. Curtidor · M. Vanegas · M. A. Patarroyo
Universidad del Rosario, Carrera 24 No. 63C-69, Bogotá, Colombia

M. E. Patarroyo
Universidad Nacional de Colombia, Carrera 45 No. 26-85, Bogotá, Colombia

## Introduction

Pulmonary tuberculosis (TB) caused by *Mycobacterium tuberculosis* remains a major public health problem worldwide. Even though the directly observed antibiotic treatment offers an effective strategy to control this disease, global efforts to control TB have faced notable difficulties for guaranteeing opportune diagnostic and drug accessibility to the poorest population. Despite the global availability of BCG vaccination, multiple factors, such as its partial protective efficacy, added to the increased risk of immunodeficient individuals to develop TB, the emergence of multi-drug-resistant strains (MDR) and extreme drug-resistant strains (XDR) have contributed to spread this disease, stressing the urgent need for finding new therapeutic and immunoprophylactic alternatives to control TB (Warner and Mizrahi 2006; WHO 2009).

One additional problem is that *M. tuberculosis* has the capacity to remain viable within the infected host for long periods of time. Infection is initiated when a potential host inhales droplet nuclei (aerosols), containing a small number of *M. tuberculosis* bacilli (Kaufmann 2001). Once in

the lungs, bacilli are internalized through phagocytosis by the resident alveolar macrophages. Appropriately activated alveolar macrophages can effectively transfer the phagocytosed bacilli to the destructive environment of lysosomes, but some bacilli are able to escape lysosomal delivery and survive within the macrophage (Armstrong and Hart 1975; Kaufmann 2001; Russell 2001). Infected macrophages can then either remain in the lung or disseminate to other body organs. However, only a 10% of infected people develop TB, because in most healthy individuals, the immune system is sufficient to keep *M. tuberculosis* in check so that disease cannot develop (WHO 2009).

*M. tuberculosis* phagocytosis by macrophages proceeds through a series of membrane invagination, budding, and fusion events that result in the formation of the phagosome (Aderem and Underhill 1999). *M. tuberculosis* entry into macrophages can occur by an array of different receptor molecules, including complement receptors, mannose receptor, the dendritic cell-specific intercellular adhesion molecule (ICAM)-3-grabbing nonintegrin (DC-SIGN), and Fc receptors (Cambi et al. 2005; Ernst 1998; Greenberg et al. 1999). The ability of multiple receptor molecules to internalize *M. tuberculosis* in macrophages is likely related to the complex structure of *M. tuberculosis* cell surface (Brennan and Nikaido 1995). The precise receptor involved in phagocytic entry may have a major impact on bacilli survival inside the macrophage.

On the other hand, proteins secreted across the cytoplasmic membrane could be involved in cell wall biogenesis, contributing to virulence or being highly antigenic (Wiker et al. 2000). The characterization of novel secreted mycobacterial proteins is fundamental in understanding the microorganism pathogenesis. *M. tuberculosis* H37Rv proteome contains over 400 potentially secreted proteins and most of them are uncharacterized to date. Among these secreted proteins, there is a family of enzymatic proteins identified by bioinformatic analyses and known as cutinase-like proteins (CULPs).These CULPs have been shown to be functionally diverse, depending on the length of the substrate hydrocarbon chain. However, none of these CULPs has cutinase activity, which has led to suggest that they play a different role in mycobacterial biology (West et al. 2009).

Cutinases (serine esterases) have been associated with fungi ability to penetrate the plant cuticle (Schafer 1993). Although *M. tuberculosis* does not find cutin, it has maintained seven putative cutinases known to cleave phospholipids in a PLA (phospholipase A)-type form, and also hydrolyze Tween. The PLA/cutinase activity could have been conserved in mycobacteria because it plays an important role in mycobacterial lipid metabolism (cell wall synthesis or nutrition), and thus pathogenesis (Parker et al. 2007).

The use of bidimensional electrophoresis allowed the identification of *M. tuberculosis* Rv2301 protein (also known as CFP25) in culture filtrate. Rv2301 contains the conventional catalytic cutinase proteins triad, formed by Ser, Asp and His (which correspond to residues Ser-123, Asp-189 and His-207 in Rv2301), with the serine residue within the conserved pentapeptide G-X-S-X-G (residues 121–125) (Weldingh et al. 1998). Rv2301 induces high IFN-$\gamma$ levels in *M. tuberculosis*-infected mice and TB patients, as well as a high delayed-type hypersensitivity (DTH) response, similar to other culture filtrate proteins known to promote high levels of protective immunity in animal models. Significant levels of protection in mice have been induced using the *clap2* plasmid, as shown by the reduction in bacterial load in lungs, as compared to mice immunized with control plasmid (West et al. 2008). In addition, Rv2301 has shown to confer a significant level of protection when tested in a multicomponent anti-TB vaccine (Sable et al. 2005).

Rv2301 contains a characteristic signal sequence (SS), which is only present in trace amounts of *M. tuberculosis* short-term culture filtrates. This study reports *rv2301* presence and transcription in *M. tuberculosis* complex members. Its localization was assessed by immunoelectron microscopy using antisera obtained against peptides derived from this protein, and detecting the protein on *M. tuberculosis* H37Rv bacilli surface. Furthermore, peptides binding with high affinity to A549 alveolar epithelial cell from carcinoma and macrophages derived from human histolytic lymphoma U937 monocytes were identified in Rv2301 amino acid sequence through a highly sensitive and robust methodology. Also, the effect of these peptides on *M. tuberculosis* entry into target cells was assessed.

## Materials and methods

### Mycobacterial strains

ATCC and Trudeau Mycobacterial Collections (TMC) were the sources of mycobacterial strains used in this study (Fig. 1), except for *M. microti* which was provided by Dr. Portaels from the Institute of Tropical Medicine (Antwerp). All mycobacterial strains were grown in a Middlebrook 7H9 medium (Difco, Detroit MI), supplemented with OADC (oleic acid, albumin, dextrose, and catalase) (BBL, BD, Sparks MD), according to the recommendations for each strain and manipulated in a biosafety level 3 facility.

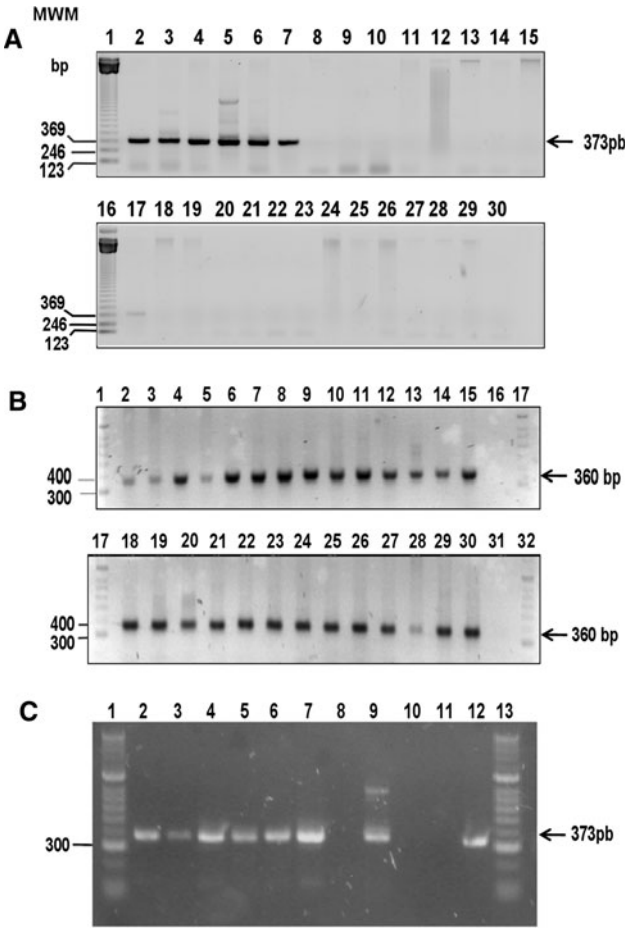


◀ **Fig. 1** **a** Rv2301 PCR product amplified from genomic DNA isolated from different mycobacterial species and strains. *1 MWM* molecular weight marker (1 kb), *2 M. tuberculosis* H37Rv (ATCC 27294), *3 M. tuberculosis* H37Ra (ATCC 25177), *4 M. bovis* (ATCC 19210), *5 M. bovis BCG* (ATCC 35734, Pasteur substrain), *6 M. africanum* (ATCC 25420), *7 M. microti* (Pasteur strain, kindly donated by Dr. F. Portaels, Institute of Tropical Medicine, Belgium, Antwerp), *8 M. flavescens* (ATCC 14474), *9 M. fortuitum* (ATCC 6841), *10 M. szulgai* (ATCC 35799), *11 M. peregrinum* (ATCC 14467), *12 M. phlei* (ATCC 11758), *13 M. scrofulaceum* (ATCC 19981), *14 M. avium* (ATCC 25291), *15 M. smegmatis* (ATCC 14468), *16* MWM (1 kb), *17 M. nonchromogenicum* (ATCC 19530), *18 M. simiae* (TMC 25275), *19 M. intracellulare* (ATCC 13950), *20 M. gastri* (ATCC 15754), *21 M. kansasii* (ATCC 12478), *22 M. diernhoferi* (ATCC 19340), *23 M. gordonae* (ATCC 14470), *24 M. marinum* (ATCC 927), *25 M. terrae* (ATCC 15755), *26 M. chelonae*-chelonae (ATCC 35752), *27 M. xenopi* (ATCC 35841), *28 M. vaccae* (ATCC 15483), *29 M. triviale* (ATCC 23292), and *30* PCR negative control. **b** *rpoB* gene amplification from genomic DNA isolated from all species and strains included in this study, as shown by a 360-bp band amplification, confirming that the DNA quality was acceptable for PCR assays. *1 MWM* molecular weight marker (1 kb), *2 M. tuberculosis* H37Rv (ATCC 27294), *3 M. tuberculosis* H37Ra (ATCC 25177), *4 M. bovis* (ATCC 19210), *5 M. bovis BCG* (ATCC 35734, Pasteur substrain), *6 M. africanum* (ATCC 25420), *7 M. microti* (Pasteur strain, kindly donated by Dr. F. Portaels, Institute of Tropical Medicine, Belgium, Antwerp), *8 M. flavescens* (ATCC 14474), *9 M. fortuitum* (ATCC 6841), *10 M. szulgai* (ATCC 35799), *11 M. peregrinum* (ATCC 14467), *12 M. phlei* (ATCC 11758), *13 M. scrofulaceum* (ATCC 19981), *14 M. avium* (ATCC 25291), *15 M. smegmatis* (ATCC 14468), *16* PCR negative control, *17* MWM (1 kb), *18 M. nonchromogenicum* (ATCC 19530), *19 M. simiae* (TMC 25275), *20 M. intracellulare* (ATCC 13950), *21 M. gastri* (ATCC 15754), *22 M. kansasii* (ATCC 12478), *23 M. diernhoferi* (ATCC 19340), *24 M. gordonae* (ATCC 14470), *25 M. marinum* (ATCC 927), *26 M. terrae* (ATCC 15755), *27 M. chelonae*-chelonae (ATCC 35752), *28 M. xenopi* (ATCC 35841), *29 M. vaccae* (ATCC 15483), *30 M. triviale* (ATCC 23292), *31* PCR negative control and *32* MWM (1 kb). **c** 373-bp Rv2301 RT-PCR product amplified from different mycobacterial species and strains. *1 MWM* molecular weight marker (200 line—Bioline, London, UK), *2 M. tuberculosis* H37Rv plus synthesis, *3 M. tuberculosis* H37Rv minus synthesis, *4 M. tuberculosis* H37Ra plus synthesis, *5 M. tuberculosis* H37Ra minus synthesis, *6 M. bovis* plus synthesis, *7 M. bovis* minus synthesis, *8 M. bovis BCG* plus synthesis, *9 M. bovis BCG* minus synthesis, *10 M. africanum* plus synthesis, *11 M. africanum* minus synthesis, *12 M. microti* plus synthesis, *13 M. microti* minus synthesis, *14* PCR positive control (*M. tuberculosis* H37Rv DNA), and *15* PCR negative control

## DNA extraction and PCR amplification

Chromosomal DNA was isolated from mycobacterial strains by phenol–chloroform extraction, as described elsewhere (Del Portillo et al. 1991; Mahairas et al. 1996; Parra et al. 1991). DNA was suspended and conserved in 1× TE buffer. PCR assays were carried out on a Perkin–Elmer Thermal Cycler GeneAmp PCR system 9600 by incubating 100 ng of genomic DNA with a PCR mixture containing: 1.5 U *Taq* polymerase (Promega), 1× *Taq* polymerase reaction buffer, 1.5 mM $MgCl_2$, 0.1 mM dNTPs and 0.4 μM of forward (3′-CTGCCCCGACGCC GAAG-5′) and reverse primers (5′-GCCGACCCACT GACTGC-3′) targeting the *Rv2301* gene. PCR amplification was carried under the following thermocycling conditions: an initial denaturation at 94°C for 5 min, followed by 30 cycles of 30 s at 94°C, 15 s at 58°C, and 15 s at 72°C. A final extension step was carried out at 72°C for 5 min. Amplified products were electrophoretically separated in 1% SYBR-safe stained agarose gels (Invitrogen, Eugene, Oregon). Distilled water and *M. tuberculosis* H37Rv DNA were used as PCR negative and positive controls, respectively. Amplification of the *rpoB* gene encoding RNA polymerase subunit B (which is present in all mycobacterial strains) was assessed as a control of DNA integrity (forward 3′-TCAAGGAGAAGC GCTACGA-5′ and reverse 5′-GGATGTTGATCAGGGTCTGC-3′) (Lee et al. 2000).

## RNA isolation and RT-PCR

Bacterial pellet was suspended in an equal volume of GTC (4 M guanidine isothiocyanate, 0.5% sodium n-lauroyl sarcosine, 25 mM TRIS sodium citrate and 0.1 M 2-mercaptoethanol) to maintain RNA integrity. Samples were homogenized and centrifuged at 1,000 rpm for

10 min at room temperature. Total RNA was isolated from the pellet by adding 1 mL TRIZOL® Reagent (Invitrogen, Carlsbad, CA) following the manufacturer's instructions, then treated with DNAse I (Invitrogen) and used as template for RT-PCR assays.

Complementary DNA (cDNA) synthesis was carried out using SuperScript™ III Reverse Transcriptase (Invitrogen) following to the manufacturer's instructions and random hexamers were used for the first-strand cDNA synthesis. In addition, the SuperScript III enzyme was replaced with DEPC-treated water in each sample as a minus control. 5 µL of cDNA were used as template for PCR amplification following the same conditions previously described for DNA. DNase- and RNase-free water and *M. tuberculosis* H37Rv DNA were used as negative and positive PCR controls, respectively. *rpo* B gene transcription was assessed as positive control (Lee et al. 2000).

## Antibodies obtained through goats immunization

Two goats, previously determined to be nonreactive to *M. tuberculosis* sonicate by Western blot, were independently inoculated with 5 mg of polymerized peptide 28458 ($CG^{52}$FARGRFEPPGIGTVGNAFVS$^{71}$GC) or polymerized peptide 28460 ($CG^{192}$THPADPNTWEANWPQHLAGAY$^{211}$GC) (Andreu et al. 1994). Prior to the immunization, peptides were emulsified in Freund's incomplete adjuvant (FIA). Animals were immunized on days 0, 20 and 40, and finally bled on day 60. Peptide sequences chosen for immunizing goats were selected based on an Rv2301 sequence analysis, using the BepiPred 1.0b Server epitope prediction software available at http://www.cbsdtu.dk/services/BepiPred/.

## SDS-PAGE and immunoblotting

Proteins from *M. tuberculosis* sonicate (30 W for 30 min in a Branson Sonifier, VWR Scientific, Boston, MA) and cellular fractions were separated by SDS-PAGE (10–20% acrylamide gradient), and then transferred to a nitrocellulose membrane using the semidry blotting technique (Kyhse-Andersen 1984). Sera obtained from goats immunized with polymerized peptides (1:100 dilution) were used as primary antibody. Sera were diluted in TBST (0.02 M Tris–HCl pH 7.5, 0.05 M NaCl, 1% Tween 20) and 5% skimmed milk. After five washes with TBST, sera were incubated for 1 h with alkaline phosphatase conjugated anti-goat IgG antibody (ICN Biomedicals, CA, USA), in a 1:3,000 dilution. Color development was assessed after using the NBT/BCIP detection kit (KPL, Gaithersburg, MD, USA).

## Immunoelectron microscopy

Immunoelectron microscopy studies were carried out using a Hitachi Hu-12A Electron Transmission microscopy. In brief, a *M. tuberculosis* H37Rv wet pellet was fixed with a 4% paraformaldehyde/0.5% glutaraldehyde solution for 2 h at 4°C. After being fixed, the pellet was dehydrated in graded ethanol (70–100% twice), and then embedded in LR white resin (Sigma) using a specific cold polymerization accelerator. Ultrathin sections were fixed on 300-mesh nickel grids coated with collodion support. Grids were blocked with 5% bovine serum albumin/0.1% Tween 20 for 1 h, and subsequently incubated at 4°C overnight with a 1:20 dilution of primary antibody. Grids were then incubated with anti-goat antibody coupled to 10-nm colloidal gold particles for 1 h at room temperature (Wagner et al. 1995). Finally, 6% uranyl acetate was added to enhance image contrast.

## Cell culture

Two cell lines obtained from the ATCC (Rockville, MD) were selected for carrying out binding assays: the A549 adherent cell line derived from human lung carcinoma (ATCC CLL-185) and the U937 monocyte cell line derived from human histolytic lymphoma (ATCC CRL-2367). A549 and U937 cells were grown in RPMI 1640 broth (Gibco) supplemented with 10% fetal bovine serum (FBS; Hyclone) (Passmore et al. 2001). Cells were dislodged using cell dissociation solution non-enzymatic 1× (Sigma), collected and washed with PBS.

## Peptide synthesis

In this study, 12 non-overlapping 20-mer-long peptides corresponding to *M. tuberculosis* Rv2301 amino acid sequence (cut2 or CFP25), were synthesized by the solid-phase multiple peptide system (Houghten 1985; Merrifield 1963; Tam et al. 1983). Only peptide 36507 overlapped peptide 30955 by 15 residues. This occurred because peptides were initially synthesized based on the Rv2301sequence reported in GenBank under the accession number NP_216817, but this sequence was annotated without the N-region of the signal sequence (first five amino acids). The complete sequence was later annotated under the GenBank Accession number NP_216817.2. Peptides identity and purity were analyzed by MALDI-TOF mass spectrometry and analytical reverse-phase high-performance liquid chromatography (RP-HPLC). A Tyr residue was added to the C-terminus of peptides which did not contain it, to enable radiolabeling.

### Radiolabeling

$^{125}$I-radiolabeling was carried out according to the previously described techniques (Hulme 1993; Weiland and Molinoff 1981; Yamamura and Kuhar 1978). Briefly, chloramine T (2.25 mg/mL) and $Na^{125}I$ (3.2 μL; 100 mCi/mL) were added to 5 μL of peptide solution (1 μg/μL). 15 μL of sodium bisulfite (2.75 mg/mL) and 50 μL of NaI (0.16 M) were added, after allowing the reaction to elapse for 5 min at 18°C. Radiolabeled peptides were then separated from reaction byproducts on a Sephadex G-10 column (80 × 5.0 mm; Pharmacia, Uppsala, Sweden).

### Binding assays

The U937 or A549 cell lines ($\sim 1.5 \times 10^6$ cells) were incubated for 90 min at 4°C with increasing amounts of each $^{125}$I-radiolabeled peptide (between 0 and 950 nM) in the presence or absence of 40 μM of unlabeled peptide to determine binding specificity (final volume: 100 μL). After incubation, unbound peptides were removed from cells by sedimentation through a dibutylphthalate-dioctylphthalate cushion mixture ($d = 1.015$ g/mL) and centrifuged at 9,000*g* for 2 min (Patarroyo et al. 2008; Plaza et al. 2007; Vera-Bravo et al. 2005). Cell-bound peptides were measured in an automatic gamma counter. The assay was carried out in triplicate under identical conditions. Mean results of triplicate assays are calculated and plotted.

### Determining binding constants

Saturation binding assays were carried out with each peptide that showed to have high specific-binding activity to target cells. To determine binding specificity of these peptides, $1.2 \times 10^6$ U937 cells were incubated for 90 min at 4°C, with increasing concentrations of radiolabeled peptide (100–4,000 nM) in a final 120 μL volume, in the presence or absence of 30 μM of unlabeled peptide. The amounts of bound and unbound peptide were determined using a gamma counter. The curves obtained were analyzed by Scatchard analysis and affinity constants were determined by a Hill equation analysis (Hulme 1993; Weiland and Molinoff 1981).

### Mycobacterial invasion assays

Invasion inhibition assays were performed according to a previously reported methodology (Bermudez and Goodman 1996; Chapeton-Montes et al. 2008a, b) with some modifications. In brief, bacteria were harvested, and then labeled using 20× SYBR-safe and stored at −20°C until use. A549 cells and U937 monocyte-derived macrophages ($1 \times 10^6$ cells), suspended in a RPMI 1640 medium and supplemented with 10% FBS, were independently seeded in 6-well multiwell plates and incubated for 16 h at 37°C under a 5% $CO_2$ atmosphere. Different peptide concentrations (5, 50 and 100 μM) were added to cell monolayers, and plates were kept at 37°C for 1 h. Cell monolayers were incubated with an RPMI 1640 medium instead of peptide as an invasion control, and with 3 μM of cytochalasin D as negative control. Mycobacteria ($1 \times 10^7$ bacilli) suspended in 300 μL of RPMI medium without antibiotics were added to each well at a 1:10 multiplicity of infection (MOI), and incubated for 16 h at 37°C. Samples were incubated with amikacin (20 μg/mL) for 2 h at 37°C. Extracellular bacilli were removed by washing wells with Hank' balanced salt solution (HBSS) thrice, and cell monolayers were dislodged using a 0.6% trypsin 0.2% EDTA solution (both from Sigma). Infected cells were suspended in 50 μL of RPMI 1640 medium and incubated with methylene blue (Merck, Germany) for 5 min, to carry out flow cytometry analyses. Data were statistically analyzed by applying a Student's *t* test.

### Latex bead internalization

Latex bead internalization assays were carried out according to a previously reported methodology (El-Shazly et al. 2007). Briefly, A549 cells ($1 \times 10^6$) were seeded on 6-well multiwell plates until forming cell monolayers. Separately, each peptide was coupled to fluorescent latex beads (Sigma). Peptide-coated beads were incubated with A549 cells at 37°C for 3 h. Non-internalized beads were removed, and cells were dislodged from cell monolayers to determine the percentage of internalized beads by FACScan flow cytometry analysis. Uncoated beads were used as negative control. To establish the peptide effect on the membrane, an additional control was performed consisting of incubating cells with each peptide suspension for 2 h, and then for 1 h with naked latex beads; finally, the percentage of internalized beads was determined by FACScan flow cytometry analysis.

### Circular dichroism (CD) spectroscopy

A possible correlation between Rv2301 HABPs function and their conformational structure was analyzed by circular dichroism (CD) analysis. CD spectra were recorded for each HABP at 20°C on a Jasco J-810 spectropolarimeter at wavelengths ranging from 260 to 190 nm in 1.00-cm cuvettes (Provencher and Glockner 1981). Peptides (0.1 mM) were dissolved in pure water or aqueous 30% (*v*/*v*) TFE. Each spectrum was obtained by averaging three scans taken at a 20-nm/min scan rate, with 1 nm spectra bandwidth and corrected for baseline deviation. The results were expressed as mean residue ellipticity [$\theta$], the units

being degrees centimeters squared per decimole, according to the function $[\theta] = \theta\lambda/(100lcn)$, where $\theta\lambda$ is the measured ellipticity, $l$ the optical path length, $c$ is the peptide concentration, and $n$ the number of amino acid residues in the peptide sequence (Sreerama et al. 1999). Using the self-optimized prediction method from alignment (SOPMA), a prediction for Rv2301 protein secondary structure was obtained (Geourjon and Deleage 1995).

## Results and discussion

Through the use of receptor-ligand assays and chemically synthesized peptides derived from *M. tuberculosis* proteins, our institute proposes a new methodology for identifying antigens capable of inhibiting in vitro the entry of *M. tuberculosis* into target cells that could be considered in the design of a subunit-based antituberculosis vaccine (Patarroyo et al. 2010; Patarroyo and Patarroyo 2008).

Although the publication of the *M. tuberculosis* H37Rv complete genomic sequence (Cole et al. 1998) has enabled important advances in the general knowledge of this pathogen's physiology, the functions, as well as the cellular localization of many of its proteins remain unknown. Among these proteins are the members of the *M. tuberculosis* cutinase family, which have been the target of research as new promising antigens with prophylactic potential against TB, due to their important role in the bacilli–host cell interactions (West et al. 2008, 2009).

In this study, the presence of the 373-bp fragment encoding Rv2301 was assessed in 27 mycobacterial strains by PCR (Fig. 1a), detecting the gene in all strains and species belonging to the *M. tuberculosis* complex (*M. tuberculosis* H37Rv, *M. tuberculosis* H37Ra, *M. bovis*, *M. bovis* BCG, *M. africanum* and *M. microti*). Amplification of the *rpoB* gene from genomic DNA was detected in all species and strains included in this study, therefore showing that the DNA was of acceptable quality for PCR assays (Fig. 1b). RT-PCR was performed on all strains that displayed a positive PCR amplification on genomic DNA to determine whether the *rv2301* gene was being transcribed under 7H9 culture medium conditions. A 373-bp fragment was observed in cDNA plus synthesis of all *M. tuberculosis* complex strains (*M. tuberculosis* H37Rv, *M. tuberculosis* H37Ra, *M. bovis*, *M. bovis* BCG, *M. africanum*, and *M. microti*). No amplification of the minus control is an indicator that there is no contamination with gDNA (Fig. 1c).

The expression of Rv2301 was confirmed employing polyclonal sera from goats inoculated with peptides 28458 and 28460. The expression of Rv2301 was confirmed using goats' polyclonal sera inoculated with peptides 28458 and 28460. Figure 2 shows the identification of a 22.5 kDa band in *M. tuberculosis* H37Rv lysate, which is consistent with Rv2301 theoretical weight in (22.6 kDa) when this protein has not been processed and is attached to the mycobacterial envelope (Parker et al. 2007). The same antibodies recognized a molecule on the surface of *M. tuberculosis* H37Rv by IEM (Fig. 3), most of colloidal gold particles were located in the bacillus envelope and some of them were located in the cytosol, but in a lower proportion, therefore, suggesting that it is possible to find a significant portion of the protein on the mycobacterial membrane, and also that the protein could be involved in protein–protein interactions with the host cell.

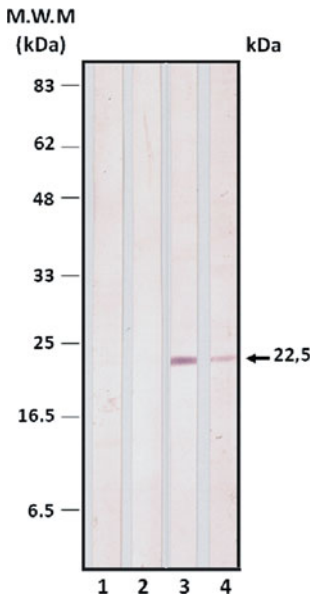


**Fig. 2** Rv2301 protein recognition. Western blotting with goats' sera inoculated with the polymerized Rv2301-derived peptides 28458 and 28460, showing immunoreactivity to *M. tuberculosis* H37Rv sonicate. *Lanes 1* and *2* pre-immune sera, *lane 3* post III/20 sera raised against peptide 28458, and *lane 4* post III/20 sera raised against peptide 28460. Post III immunization sera showed a weak recognition of a 22.5-kDa protein

Receptor–ligand assays using radiolabeled synthetic peptides were carried out to determine which of the sequences of Rv2301 bind specifically to U937 and A549 cell in vitro. Peptides binding activity was determined as the ratio between specific binding and total peptide added. Specific binding activity was defined as the slope of the specific binding curve (specific binding = total binding–nonspecific binding) between the amount of radiolabeled peptide binding specifically to A549 and U937 cells and peptide added at four increasing concentrations. Five of the twelve synthetic peptides spanning the entire sequence length of Rv2301 showed high binding activity to A549 and U937 cells (30958, 30960, 30963, 30965 and 36507) and were therefore classified as HABPs, while peptides 30959 and 30964 showed high binding activity to A549

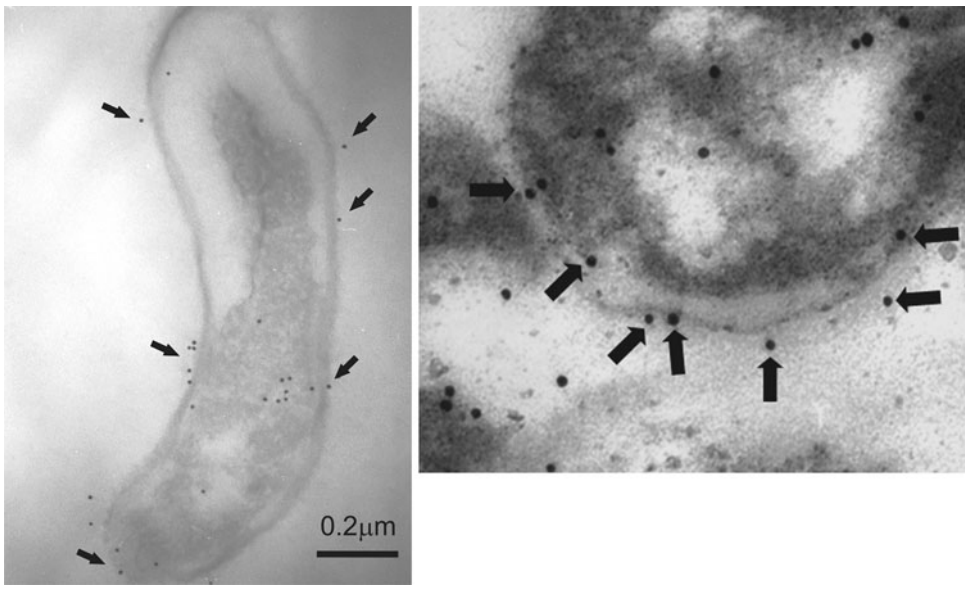


**Fig. 3** Immunoelectron microscopy. Goat antibodies raised against polymerized peptides showed recognition of the putative protein encoded by the *Rv2301* gene in *M. tuberculosis* H37Rv bacilli surface (10 nm gold-labeled anti-goat IgG are indicated by *arrows*)

cells only (Fig. 4). Rv2301 HABPs were mainly distributed along the entire protein sequence; however, two specific binding regions could be distinguished for A549 cells, spanning amino acids 72–131 and 172–230.

Interactions between Rv2301 HABPs and target cell surface receptors were characterized by saturation assays with U937 cells (Fig. 5). Accordingly, HABPs established high affinity interactions with a large number of binding sites on the surface of U937 cells (~1–3 million binding sites per cell). These binding interactions had dissociation constants within the nanomolar range (approximately 800 nM), as well as strong positive cooperativity ($n_H > 1$). Nevertheless, these assays only provide a preliminary insight about the nature of the molecules which interact with Rv2301 HABPs; further studies are needed to completely identify these possible receptors.

The possible biological importance of the HABPs identified in Rv2301 in mediating *Mycobacterium*–host cell interactions was analyzed according to a methodology previously reported by our institute (Chapeton-Montes et al. 2008a, b; Patarroyo et al. 2008; Plaza et al. 2007; Vera-Bravo et al. 2005). As shown in Fig. 6a, the results

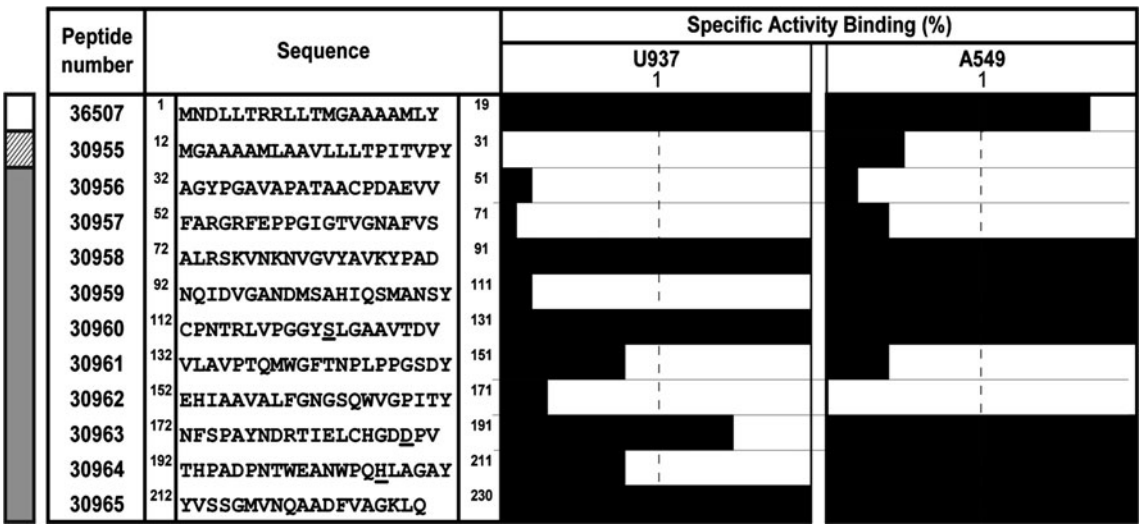


**Fig. 4** Rv2301-derived peptides cell binding activity profile. 20-mer-long peptides spanning the entire Rv2301 protein sequence were synthesized and assessed in specific binding assays with A549 and U937 cells. A Tyr residue was added to the C-terminus of those peptides which did not contain it in their sequence. *Black bars* represent each peptides binding activity. Peptides having a specific binding activity ≥1% were classified as HABPs. Rv2301 topology is presented on the *left hand side*. *Shaded regions* show the transmembrane domain present in the Rv2301 sequence, *dark gray* regions corresponds to the outside domain and *white regions* corresponds to inner domain (N-terminal). Catalytic triad residues are underlined

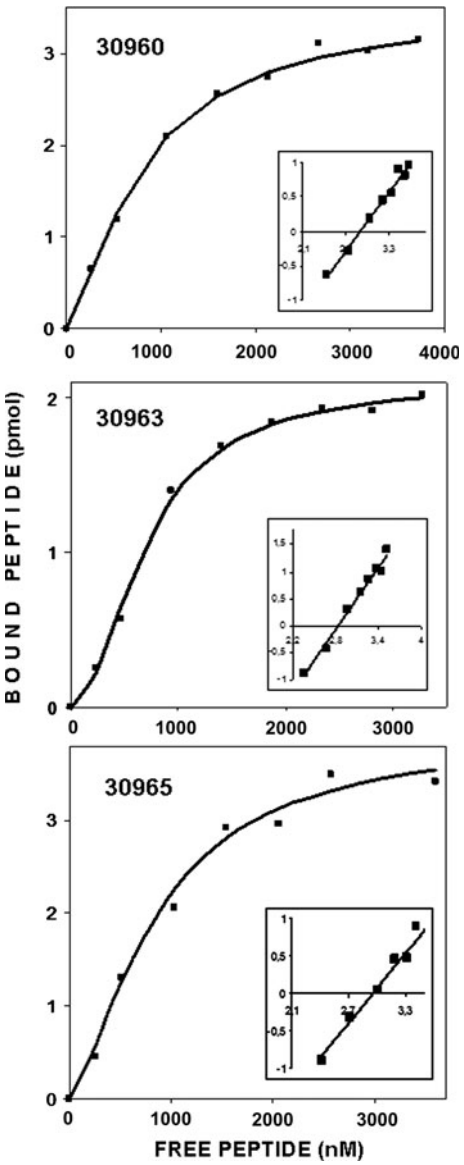


**Fig. 5** Saturation curves for HABPs 30960, 30963 and 30965, which bind with high activity to U937 cells. Saturation curves were obtained by plotting the amount of specifically bound $^{125}$I-HABP against the amount of free $^{125}$I-HABP. Affinity constants and the maximum number of sites per cell were obtained from these curves by Hill analysis. *Inset* the abscissa is Log *F* in the Hill Plot and the ordinate is Log[$B/B_m - B$], being $B_m$ the maximum amount of bound peptide, *B* the bound peptide and *F* the free peptide

obtained from invasion inhibition assays with A549 and U937 cells showed that all the HABPs tested inhibited the entry of *M. tuberculosis* H37Rv into these two cell lines in vitro, even at the smallest peptide concentration (5 μM). Only HABPs 36507 and 30959 showed an entry inhibition dependent on the peptide concentration, for the remaining HABPs there is a variable relation between concentration and inhibition. These results are relevant taking into account that a single peptide is being able to significantly reduce invasion of target cells. However, further studies are needed in order to determine whether these inhibitory HABPs have also a potential immunomodulatory effect.

The involvement of the HABPs identified in Rv2301 in host cell invasion was further evaluated by determining their ability to facilitate internalization into A549 cell, when being coupled to fluorescent latex beads. As it can be observed in Figs. 6b, 7 the highest internalization percentage was observed when latex beads were coated with HABP 36507, while inhibition with HABP 30959 showed a similar percentage to that observed with naked beads. However, when cells were incubated first with the suspension of each HABP and then with naked latex beads, small internalization percentages were found for all HABPs, which were even smaller than the one shown by the bead internalization control (latex beads).

The ability of the HABPs identified in the Rv2301 sequence to inhibit invasion of *M. tuberculosis* H37Rv into to target cells, suggests that active and specific binding to cell surface receptors prevents entrance of *M. tuberculosis* through this invasion pathway. Such hypothesis is further supported by the results of internalization assays carried out with peptide-coated latex beads and epithelial cells, where peptide-coated beads were more actively internalized than non-coated beads. Particularly, HABP 36507 showed the largest inhibition percentage and displayed the highest internalization percentage.

CD spectroscopy was used for assessing HABPs secondary structures; peptides 36507 and 30965 showed structural elements characteristic of α-helices, recognized by two characteristic minima in 208 and 222 nm, and a maximum in 195 nm, whereas HABPs 30958, 30963 and 30960 did not show any structural elements in particular. Experimental results agree with SOPMA prediction, in which HABPs 36507 and 30965 are located in predominant α-helical regions, while the three remaining HABPs do not present defined structural elements. The results obtained in the analysis of HABPs secondary structure elements showed a good agreement with predictions established for the native protein; however, it was not possible to establish a direct relationship between the HABPs ability to inhibit invasion and their structural conformations. These analyses are of great importance, taking into account that the induction of an effective immune response is associated with the adjustment of the peptide sequence to the involved molecules, by presenting antigens to the immune system (Patarroyo et al. 2010; Patarroyo and Patarroyo 2008).

In our experience, peptides that bind specifically to target cells, and are capable of inhibiting mycobacterial entry to some extent, could be used as template for designing immunomodulating peptides. Immune responses against high specific binding sequences of mycobacterial proteins can prevent target–cell invasion, either during a

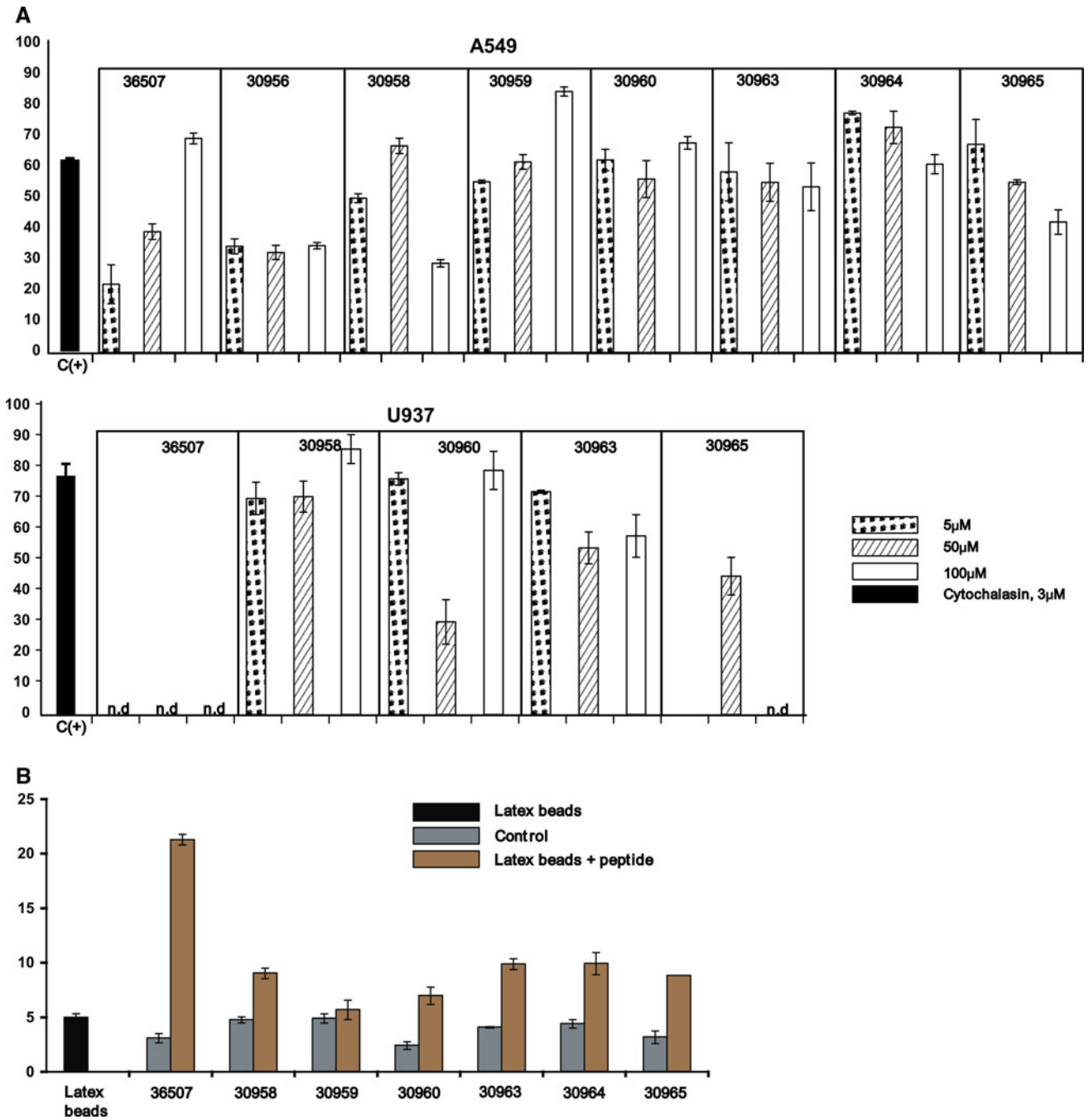


**Fig. 6** **a** Invasion inhibition assays with the Rv2301 identified HABPs. Percentages of mycobacterial invasion into A549 and U937 cell lines at different peptide concentrations. Cytochalasin D (actin polymerization inhibitor) was used as an invasion inhibition control. The results correspond to the percentage of invasion inhibition, calculated for each treatment ± standard deviation. **b** Internalization of peptide-coated beads by A549 epithelial cells. *Shaded bars* (in sepia) correspond to the percentage of HABP-coated latex beads that were internalized by A549 cells. *Dark gray bars* correspond to the percentage of latex beads that were internalized when the cell were first incubated with each HABP and then with naked latex beads (control assay). The *black bar* corresponds to internalization of non-peptide-coated beads by cells that had not been exposed to any HABP

first encounter with the pathogen or during reactivation of a latent infection (Patarroyo et al. 2010; Patarroyo and Patarroyo 2008).

In conclusion, this study shows the presence and expression of *M. tuberculosis* Rv2301 gene in all strains belonging to the *M. tuberculosis* complex, as well as the regions of the protein which are binding specifically to target cells, and are therefore capable of inhibiting host cell invasion in vitro. The results suggest an important role for these sequences in the *M. tuberculosis*–macrophage

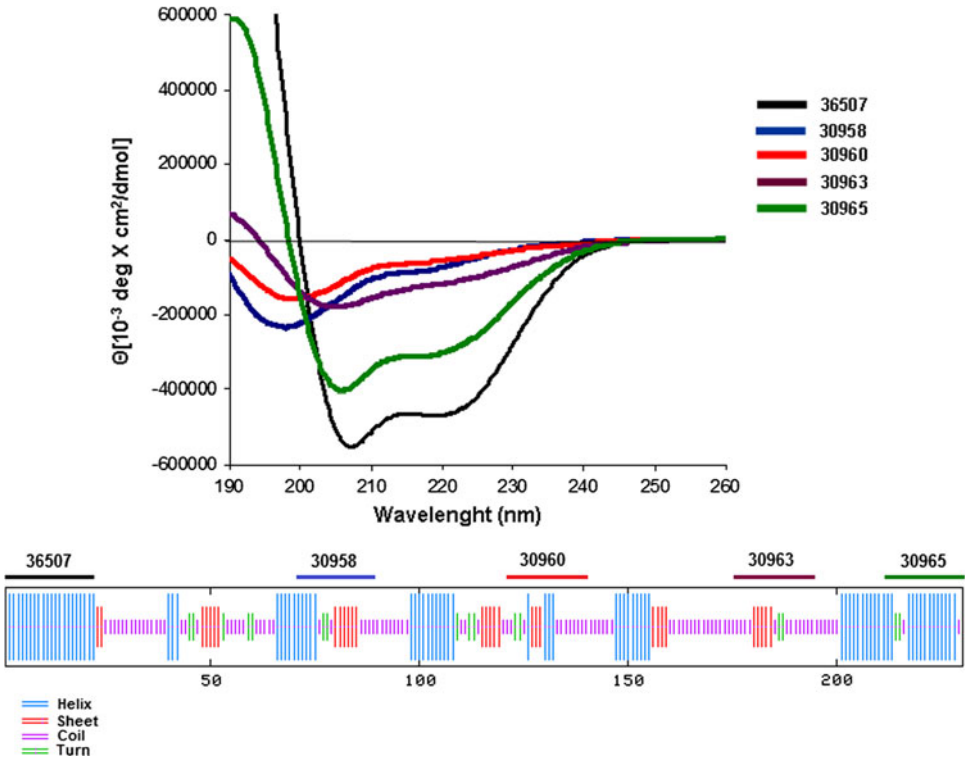


**Fig. 7** Circular dichroism (CD) spectra obtained for Rv2301 identified HABPs. Some peptides showed structural elements with low ellipticity that allowed the formation of stable secondary structures. [Θ] is the molar ellipticity per amino acid residue in the peptide, CD spectra were obtained by averaging four scans taken at 0.1-nm intervals between 260 and 190 nm at 20°C. At the *bottom* is the SOPMA prediction for Rv2301 secondary structure showing R-helical (*blue*), *β*-turn (*red*) and random coil (*violet*) elements, and the localization of Rv2301 HABPs (*horizontal bars*)

interaction and complement previous studies reported by our group (Chapeton-Montes et al. 2008b; Patarroyo et al. 2008; Plaza et al. 2007; Vera-Bravo et al. 2005). The same highly sensitive and robust methodology has been used to identify and characterize amino acid sequences mediating binding interactions with target cells, and that have the ability to inhibit mycobacterial invasion. Therefore, these sequences can be included as potential components of a subunit-based, multi-epitopic, chemically synthesized antituberculosis vaccine.

**Acknowledgments** We would like to thank Nora Martinez for translating and revising the manuscript.

**Conflict of interest** The authors declare no conflict of interest. The authors alone are responsible for the content and writing of this manuscript.

## References

Aderem A, Underhill DM (1999) Mechanisms of phagocytosis in macrophages. Annu Rev Immunol 17:593–623

Andreu D, Albericio F, Solé NA, Munson MC, Ferrer M, Barany G (1994) Formation of disulfide bonds in synthetic peptides and proteins. Methods Mol Biol 35:91–169

Armstrong JA, Hart PD (1975) Phagosome–lysosome interactions in cultured macrophages infected with virulent tubercle bacilli. Reversal of the usual nonfusion pattern and observations on bacterial survival. J Exp Med 142:1–16

Bermudez LE, Goodman J (1996) *Mycobacterium tuberculosis* invades and replicates within type II alveolar cells. Infect Immun 64:1400–1406

Brennan PJ, Nikaido H (1995) The envelope of mycobacteria. Annu Rev Biochem 64:29–63

Cambi A, Koopman M, Figdor CG (2005) How C-type lectins detect pathogens. Cell Microbiol 7:481–488

Chapeton-Montes JA, Plaza DF, Barrero CA, Patarroyo MA (2008a) Quantitative flow cytometric monitoring of invasion of epithelial cells by *Mycobacterium tuberculosis*. Front Biosci 13:650–656

Chapeton-Montes JA, Plaza DF, Curtidor H, Forero M, Vanegas M, Patarroyo ME, Patarroyo MA (2008b) Characterizing the *Mycobacterium tuberculosis* Rv2707 protein and determining its sequences which specifically bind to two human cell lines. Protein Sci 17:342–351

Cole ST, Brosch R, Parkhill J, Garnier T, Churcher C, Harris D, Gordon SV, Eiglmeier K, Gas S, Barry CE 3rd, Tekaia F, Badcock K, Basham D, Brown D, Chillingworth T, Connor R, Davies R, Devlin K, Feltwell T, Gentles S, Hamlin N, Holroyd S, Hornsby T, Jagels K, Krogh A, McLean J, Moule S, Murphy L, Oliver K, Osborne J, Quail MA, Rajandream MA, Rogers J, Rutter S, Seeger K, Skelton J, Squares R, Squares S, Sulston JE, Taylor K, Whitehead S, Barrell BG (1998) Deciphering the biology of *Mycobacterium tuberculosis* from the complete genome sequence. Nature 393:537–544

Del Portillo P, Murillo LA, Patarroyo ME (1991) Amplification of a species-specific DNA fragment of *Mycobacterium tuberculosis* and its possible use in diagnosis. J Clin Microbiol 29:2163–2168

El-Shazly S, Ahmad S, Mustafa AS, Al-Attiyah R, Krajci D (2007) Internalization by HeLa cells of latex beads coated with mammalian cell entry (Mce) proteins encoded by the mce3 operon of *Mycobacterium tuberculosis*. J Med Microbiol 56:1145–1151

Ernst JD (1998) Macrophage receptors for *Mycobacterium tuberculosis*. Infect Immun 66:1277–1281

Geourjon C, Deleage G (1995) SOPMA: significant improvements in protein secondary structure prediction by consensus prediction from multiple alignments. Comput Appl Biosci 11:681–684

Greenberg D, Hingston G, Harman J (1999) Chest wall tuberculosis. Breast J 5:60–62

Houghten R (1985) General method for the rapid solid phase synthesis of large numbers of peptides: specificity of antigen antibody interaction at the level of individual amino acid. Proc Natl Acad Sci USA 82:5131–5135

Hulme E (1993) Receptor–ligand interactions. A practical approach. IRL Press, Oxford

Kaufmann SH (2001) How can immunology contribute to the control of tuberculosis? Nat Rev Immunol 1:20–30

Kyhse-Andersen J (1984) Electroblotting of multiple gels: a simple apparatus without buffer tank for rapid transfer of proteins from polyacrylamide to nitrocellulose. J Biochem Biophys Meth 10:203–209

Lee H, Park HJ, Cho SN, Bai GH, Kim SJ (2000) Species identification of mycobacteria by PCR-restriction fragment length polymorphism of the *rpoB* gene. J Clin Microbiol 38:2966–2971

Mahairas GG, Sabo PJ, Hickey MJ, Singh DC, Stover CK (1996) Molecular analysis of genetic differences between *Mycobacterium bovis* BCG and virulent *M. bovis*. J Bacteriol 178:1274–1282

Merrifield RB (1963) Solid phase peptide synthesis. 1. The synthesis of tetrapeptide. J Am Chem Soc 85:2149–2154

Parker SK, Curtin KM, Vasil ML (2007) Purification and characterization of mycobacterial phospholipase A: an activity associated with mycobacterial cutinase. J Bacteriol 189:4153–4160

Parra CA, Londono LP, Del Portillo P, Patarroyo ME (1991) Isolation, characterization, and molecular cloning of a specific *Mycobacterium tuberculosis* antigen gene: identification of a species-specific sequence. Infect Immun 59:3411–3117

Passmore JS, Lukey PT, Ress SR (2001) The human macrophage cell line U937 as an in vitro model for selective evaluation of mycobacterial antigen-specific cytotoxic T-cell function. Immunology 102:146–156

Patarroyo ME, Patarroyo MA (2008) Emerging rules for subunit-based, multiantigenic, multistage chemically synthesized vaccines. Acc Chem Res 41:377–386

Patarroyo MA, Curtidor H, Plaza DF, Ocampo M, Reyes C, Saboya O, Barrera G, Patarroyo ME (2008) Peptides derived from the *Mycobacterium tuberculosis* Rv1490 surface protein implicated in inhibition of epithelial cell entry: potential vaccine candidates? Vaccine 26:4387–4395

Patarroyo ME, Cifuentes G, Martinez NL, Patarroyo MA (2010) Atomic fidelity of subunit-based chemically synthesized antimalarial vaccine components. Prog Biophys Mol Biol 102:38–44

Plaza DF, Curtidor H, Patarroyo MA, Chapeton-Montes JA, Reyes C, Barreto J, Patarroyo ME (2007) The *Mycobacterium tuberculosis* membrane protein Rv2560—biochemical and functional studies. Febs J 274:6352–6364

Provencher SW, Glockner J (1981) Estimation of globular protein secondary structure from circular dichroism. Biochemistry 20:33–37

Russell DG (2001) *Mycobacterium tuberculosis*: here today, and here tomorrow. Nat Rev Mol Cell Biol 2:569–577

Sable SB, Verma I, Khuller GK (2005) Multicomponent antituberculous subunit vaccine based on immunodominant antigens of *Mycobacterium tuberculosis*. Vaccine 23:4175–4184

Schafer W (1993) The role of cutinase in fungal pathogenicity. Trends Microbiol 1:69–71

Sreerama N, Venyaminov SY, Woody RW (1999) Estimation of the number of alpha-helical and beta-strand segments in proteins using circular dichroism spectroscopy. Protein Sci 8:370–380

Tam JP, Heath WF, Merrifield RB (1983) An SN2 deprotection of synthetic peptides with a low concentration of hydrofluoric acid in dimethyl sulfide: evidence and application in peptide synthesis. J Am Chem Soc 105:6442–6445

Vera-Bravo R, Torres E, Valbuena JJ, Ocampo M, Rodriguez LE, Puentes A, Garcia JE, Curtidor H, Cortes J, Vanegas M, Rivera ZJ, Diaz A, Calderon MN, Patarroyo MA, Patarroyo ME (2005) Characterising *Mycobacterium tuberculosis* Rv1510c protein and determining its sequences that specifically bind to two target cell lines. Biochem Biophys Res Commun 332:771–781

Wagner B, Fattorini L, Wagner M, Jin SH, Stracke R, Amicosante G, Franceschini N, Orefici G (1995) Antigenic properties and immunoelectron microscopic localization of *Mycobacterium fortuitum* beta-lactamase. Antimicrob Agents Chemother 39:739–745

Warner DF, Mizrahi V (2006) Tuberculosis chemotherapy: the influence of bacillary stress and damage response pathways on drug efficacy. Clin Microbiol Rev 19:558–570

Weiland GA, Molinoff PB (1981) Quantitative analysis of drug-receptor interactions: I. Determination of kinetic and equilibrium properties. Life Sci 29:313–330

Weldingh K, Rosenkrands I, Jacobsen S, Rasmussen PB, Elhay MJ, Andersen P (1998) Two-dimensional electrophoresis for analysis of *Mycobacterium tuberculosis* culture filtrate and purification and characterization of six novel proteins. Infect Immun 66:3492–3500

West NP, Wozniak TM, Valenzuela J, Feng CG, Sher A, Ribeiro JM, Britton WJ (2008) Immunological diversity within a family of cutinase-like proteins of *Mycobacterium tuberculosis*. Vaccine 26:3853–3859

West NP, Chow FM, Randall EJ, Wu J, Chen J, Ribeiro JM, Britton WJ (2009) Cutinase-like proteins of *Mycobacterium tuberculosis*: characterization of their variable enzymatic functions and active site identification. Faseb J 23:1694–1704

WHO (2009) World Health Organization Report. Global Tuberculosis Control. EPIDEMIOLOGY, STRATEGY, FINANCING

Wiker HG, Wilson MA, Schoolnik GK (2000) Extracytoplasmic proteins of *Mycobacterium tuberculosis*—mature secreted proteins often start with aspartic acid and proline. Microbiology 146(Pt 7):1525–1533

Yamamura HI ES, Kuhar MJ (1978) Neurotransmitter receptor binding. Raven Press, New York